ChemComm

Accepted Manuscript

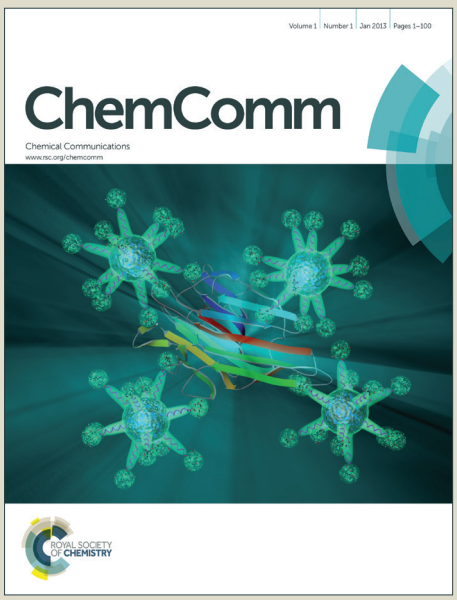

ROYAL SOCIETY OF CHEMISTRY

www.rsc.org/chemcomm

Chemical Communications ChemComm

Cite this: DOI: 10.1039/c0xx00000x

www.rsc.org/xxxxxx

FEATURE ARTICLE

Mechanochemical synthesis of advanced nanomaterials for catalytic applications

Chunping Xu[a], Sudipta De[b], Alina M. Balu[c, d], Manuel Ojeda[d] and Rafael Luque[d]*

Received (in XXX, XXX) Xth XXXXXXXXX 20XX, Accepted Xth XXXXXXXXX 20XX

DOI: 10.1039/b000000x

Mechanochemical synthesis emerged as a most advantageous, environmentally sound alternative to traditional routes for nanomaterials preparation with outstanding properties for advanced applications. Featuring simplicity, high reproducibility, mild/short reaction conditions and often solvent-free (dry milling), mechanochemistry can offer remarkable possibilities in the development of advanced catalytically active materials. The proposed contribution has been aimed to provide a brief account of remarkable recent findings and advances in the mechanochemical synthesis of solid phase advanced catalysts as opposed to conventional systems. The role of mechanical energy in the synthesis of solid catalysts and their application is critically discussed as well as the influence of the synthesis procedure on the physicochemical properties and efficiency of synthesized catalysts. The main purpose of this feature article is to highlight the possibilities of mechanochemical protocols in (nano)materials engineering for catalytic applications.

1. History and developments of mechanochemistry

Mechanochemistry deals with chemical transformations induced by mechanical means such as compression, shear, or friction. In mechanochemical processes, the energy required for the activation of chemical reactions is usually provided by mechanical force as similar to thermochemistry, photochemistry, or electrochemistry where energy is provided by heat, light, or electrical potential, respectively.

Mechanochemical processes have a long history and continue to be of high importance because these can quantitatively and rapidly promote solid-phase reactions only using nominal amounts (wet milling or liquid-assisted grinding). In conventional chemical synthesis, the solvent often plays a key role in energy dispersion, dissolution/solvation and transportation of chemicals. Mass and energy transport may be hampered in solventless reactions. The efficient mixing process under ball milling or grinding can offer an effective way out from this problem, enabling the reactions between solids or solidified reagents in solvent-free conditions.[1] Despite these advances in solvent-free molecular synthesis, solvents remain prevalent for the isolation of products in satisfactorily pure forms. "Liquid-assisted grinding" (LAG) has been introduced to provide a potential alternative to minimize the use of solvents in (nano)materials syntheses.[2] In contrast to "*dry milling*" mechanochemical processes, LAG may offer advantages such as greater time efficiency, proper usage of materials and energy and can result in the discovery of new or improved reactivity and products.

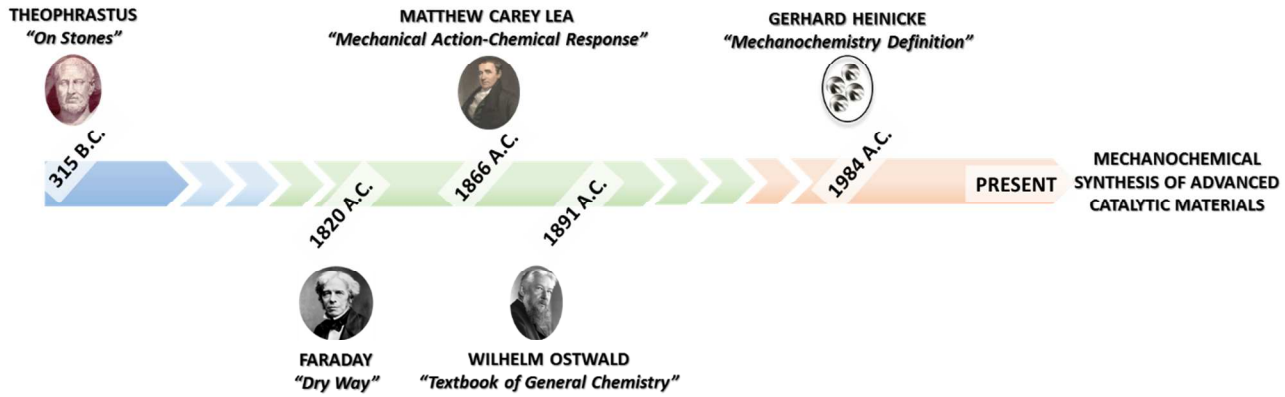

There is no detailed historical information on when and how the first mechanochemical reactions were initiated. Aristotle's student Theophrastus wrote a short booklet on ca. 315 B.C. entitled "*On Stones*" which contains a reference on the reduction of cinnabar to mercury by grinding in a copper mortar with a copper pestle, perhaps accounting for the first example of a

mechanochemical reaction.[3] After that, no such process was appropriately reported for the next 2000 years. In 1820, Faraday described the reduction of silver chloride by grinding with zinc, tin, iron and copper in a mortar.[4] He referred this process as a "*dry way*" of inducing reactions. According to his description, the reaction between silver chloride and zinc was fast and highly exothermic, raising the possibility that he actually observed a mechanochemically induced self-sustaining reaction. However, the first experiment connecting mechanical action and chemical response was reported by Matthew Carey Lea in 1866.[5] His research was extended to a considerable number of compounds and consequently was able to establish the principle that mechanical grinding can initiate chemical reactions different from commonly utilised thermochemical reactions in the same system.[6] The most remarkable finding related to the decomposition of mercuric and silver chlorides. Both compounds decomposed while triturated in a mortar, although they are known to melt or sublime undecomposed upon heating. These experiments can be considered to be the first systematic investigations on the chemical effects of mechanical actions. The term "mechanochemistry" was first introduced by Wilhelm Ostwald in the *Textbook of General Chemistry* in 1891, where mechanochemistry was considered as a part of physical chemistry such as thermochemistry, electrochemistry, sonochemistry or photochemistry. Almost a century later, Gerhard Heinicke proposed in 1984 the presently accepted definition of mechanochemistry as "*that branch of chemistry concerned with chemical and physical changes of solids induced by the action of mechanical influence*".[7]

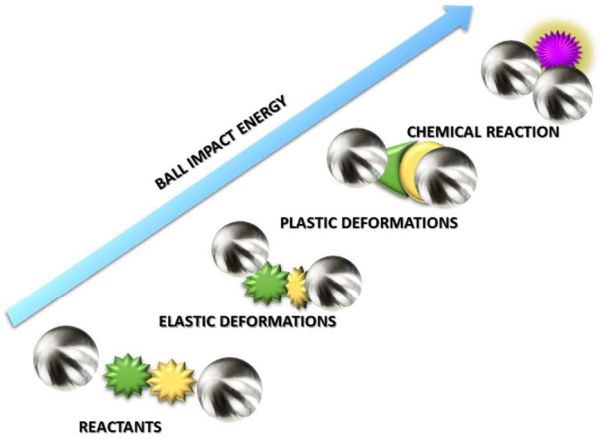

Figure 1. Mechanochemical reactions: from reactants to products.

According to IUPAC contributions, mechanochemistry is generally defined as the field of reactions caused by mechanical energy.[8] History demonstrates, once again, that mechanochemistry is not a novel concept. Most developments in mechanochemical processes and methodologies however took place in the past two decades, generally related to the application of mechanochemical processes in synthetic organic chemistry. In this regard, a significant number of reports could be found on mechanochemical reactions, indicating that a growing awareness of scientists in the field.[9] Many reports in fact provided evidences of the effectiveness and remarkable advantages of using mechanochemical syntheses in terms of cost, sustainability, and reproducibility as summarized in the recent comprehensive revision of advances, opportunities and applications of mechanochemistry by James *et al*.[9a, 10]

Interestingly, recent research endeavours re-invented the concept of mechanochemistry taking it to the next stage for the design of advanced nanomaterials with a wide range of uses and applications.[9,10] Besides classical organic synthesis, mechanochemistry can also be applied to borderline research areas between inorganic and organic chemistry including the synthesis of metal complexes,[10] metal-organic frameworks,[11] hydrogen storage materials[12] as well as the design of advanced nanocatalysts.[13] In terms of materials engineering, mechanochemical activation can provide an increase in surface area as well as surface energy of a material by altering the structure, chemical composition and/or chemical reactivity occurred throughout the milling process as well as lead to novel families of advanced materials in a simple and reproducible way. This contribution has been aimed to highlight the possibilities of mechanochemistry in the preparation and design of advanced nanomaterials for a range of catalytic applications.

2. Mechanochemical synthesis of advanced catalytic materials

The development of mechanochemical approaches for the preparation of catalysts with novel properties with improved catalyst activity and selectivity has experienced a significant evolution in recent years, with most reports available in the field over the past 5-10 years. Mechanochemistry emerged as a highly promising and simple methodology able to compete with traditional synthetic protocols for catalysts/nanomaterials syntheses which generally involve multi-step processes, heating and/or addition of expensive and hazardous reagents. Inherent disadvantages of conventional materials-synthetic protocols could be overcome using a simple grinding step under ball milling conditions. During grinding (or milling), a mixture/material accumulates an excess of potential energy which together with shear and friction forces can introduce a great variety of defects/changes in the final material which can drastically improve/modify its reactivity (Figure 1). The coming sections have been aimed to provide an overview on how mechanochemical syntheses of solid materials (mainly heterogeneous catalysts) can remarkably influence their catalytic properties for specific applications. A wide range of catalysts from supported nanoparticles to nanocomposites and similar nanomaterials have been synthesized using mechanochemical protocols as illustrated with examples in the coming sections (Scheme 1).

2.1 Supported metal nanoparticles

Mechanochemical reduction could be an effective route for the synthesis of metal nanoparticles (generally noble metals) with improved structural and catalytic properties. Mechanochemically prepared Ag/Al_2O_3 nanomaterials have been prepared and tested in the selective catalytic reduction (SCR) of NO_x using hydrocarbons in the presence and absence of hydrogen.[14] The catalyst exhibited a remarkable increase in activity at lower reaction temperatures as compared to traditional catalysts prepared via standard wet impregnation methods. The enhanced

activity of the mechanochemically synthesized catalyst related to surface modifications which provided an increased affinity towards hydrocarbons relative to water, consequently reducing the activation barrier for the reduction of NO_x. Two-dimensional NMR correlation experiments and water TPD measurements coupled with *in situ* DRIFTS analysis indicated that the active sites on the ball milled Ag catalyst remarkably promoted the formation of intermediate NCO species by increasing the hydrophobicity of both support and catalyst.

A rapid and solventless process for the bulk preparation of metal nanoparticles decorated on carbon nanotubes has been also recently described.[15] The straightforward two-step process involved a dry mixing of a precursor metal salt (*e.g.*, a metal acetate) with carbon nanotubes (single- or multiwalled) followed by heating in an inert atmosphere in the absence of any solvent, reducing agent or electric current. The proposed methodology can be in principle scalable to multigram quantities and generally applicable to various other carbon substrates (*e.g.*, carbon nanofibers, expanded graphite and carbon black) and many metal salts (*e.g.*, Ag, Au, Co, Ni and Pd acetates). In a model study, Ag nanoparticle-decorated carbon nanotube materials (Figure 2) were prepared by using various techniques, metal loading levels, thermal treatment temperatures and nanotube oxidative acid treatments. The average nanoparticle (NPs) size was found to be independent of thermal treatment but increased with metal loading, which indicated that the nanotube surface contained a constant number of nanoparticle- anchoring sites which could potentially serve to control NPs sizes by simply varying metal loadings. Interestingly, the use of mechanical mixing or oxidative acid treatment of starting MWCNTs resulted in Ag NPs with reduced sizes, most probably due to exposure of the increased number of nanotube surface-anchoring sites.

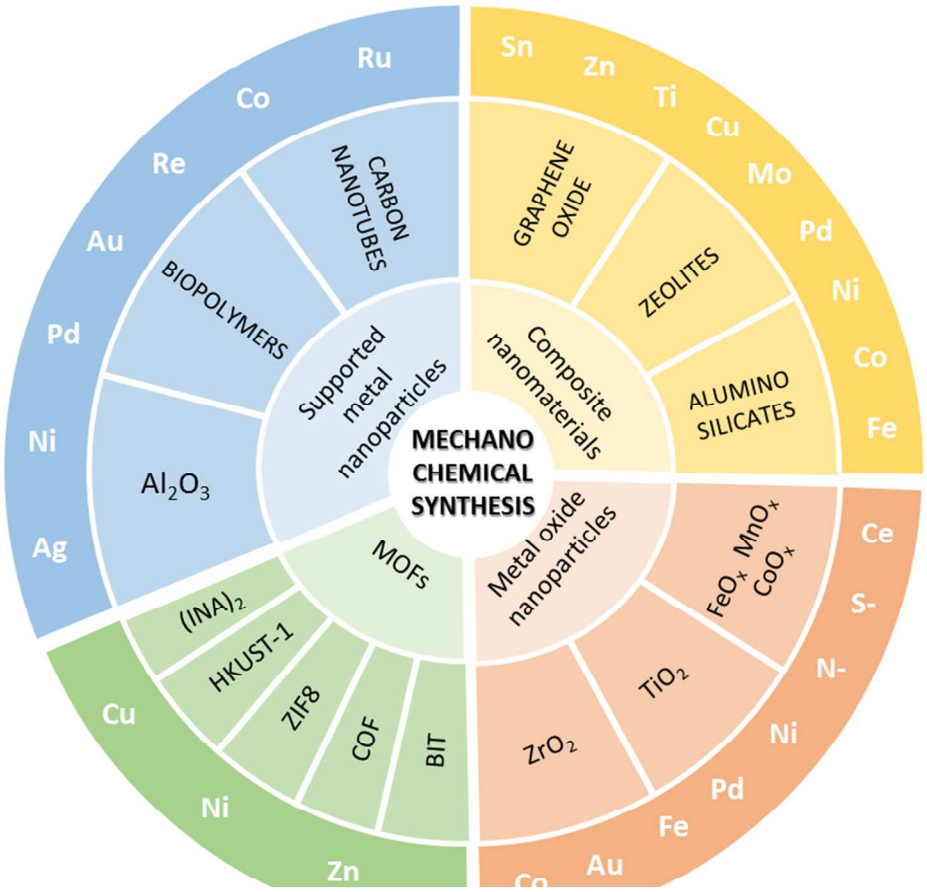

Scheme 1. Pictorial representation of different types of mechanochemically synthesized (nano)materials. From supported metal nanoparticles, composite nanomaterials to metal oxide nanoparticles and metal organic frameworks (MOFs) including covalent organic frameworks (COF). Examples of relevant materials include zinc-based ZIF-8 structures (BIT-11), $Cu(INA)_2$ and Cu-containing HKUST-1 as well as supported noble metals on aluminosilicates, graphene, etc.

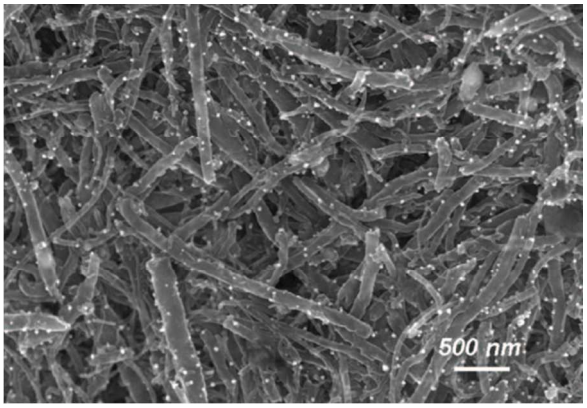

Fig. 2. SEM image of Ag nanoparticle-decorated MWCNT sample prepared *via* ball-milling process.

In situ HR-TEM studies of a CH_3COOAg/MWCNT mixture heated to 150 °C revealed the presence of intermediate CH_3COOAg/Ag^0 nano-species with two types of morphologies (droplet- and mushroom type). Mushroom-like morphologies suggested that formation of the Ag phase started away from the nanotube surface. A strong interaction of Ag NPs with MWCNTs

was revealed by Raman spectroscopy due to metal–nanotube electronic interactions. The same mix-and-heat approach could be extended for other metal acetates including Au, Co, Ni and Pd, which also successfully decorated carbon nanotubes as metal nanoparticles. Comparably, the use of iron and zinc acetates yielded the corresponding metal oxide–nanotube nanohybrids.

In a more recent report, carbon nanotubes were also utilized as support for Pd NPs using a similar solventless dry milling method in the absence of any reducing agent or electric current.[16] Pd NPs (1–3 nm size) could be uniformly dispersed on the support and the mechanochemically prepared nanocatalyst exhibited excelling activities in Suzuki cross coupling reactions with a high turnover numbers (TON) and turnover frequencies (TOF). Pd NPs prepared by thermal annealing (300 ºC) formed larger NPs due to agglomeration as compared to Pd NPs prepared at room temperature, therefore leading to reduced catalytic activities. A similar mechanosynthesis technique can be utilised to prepare functionalized ultra-small Au NPs in gram scale using a bottom-up approach.[17] The size of Au NPs could be controlled by varying the ligand/precursor ratio, milling time and/or the nature of the ligand.

Along these lines, a simple and scalable method for the preparation of supported gold, palladium and gold–palladium bimetallic catalysts via physical mixing of the acetate salts of the metals followed by a simple heat treatment was also recently described (Figure 2).[18]

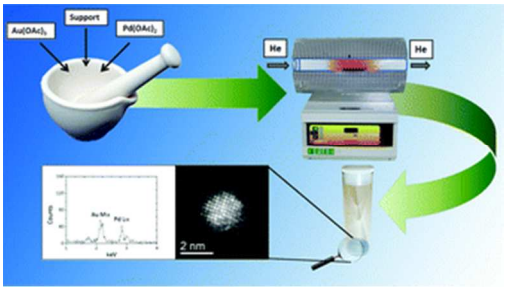

Fig. 3. Mechanochemical preparation of supported nanoparticles on various supports as advanced nanocatalysts. Reproduced with permission of the Royal Society of Chemistry from reference 18.

These types of nanocatalysts based on Au and Pd are usually prepared using chloride salt precursors; however, the complete removal of chlorides from the final catalyst is known to be very difficult. The presence of chlorides in the catalyst can lead to particle agglomeration through Au–Cl–Au bridges and also blocking of the active sites. The surface chloride concentration can be minimized by thermal treatment of the catalyst and close control of pH during synthesis but such methods often result in metal agglomeration (e.g. sintering) and reduction in Au loadings. Upon mechanochemical heat treatment under inert atmospheres, metal acetates are known to sublime before decomposing and an auto-reduction takes place which in principle directs NP sizes as well as their interaction with the support. The preparation of Au–Pd/TiO_2 and Pd/TiO_2 catalysts by physically mixing gold and palladium acetates with the support in a pestle and mortar (1–20 min) followed by heat treatment provided access to the aforementioned chlorine-free catalysts with enhanced catalytic activities. Investigations of such nanocatalysts in the oxidation of benzyl alcohol and the direct synthesis of hydrogen peroxide demonstrated that mechanochemical nanomaterials exhibited a superior activity as compared to similar catalysts prepared by impregnation and deposition–precipitation.[18] The greater activity and selectivity of the bimetallic catalyst indicates a beneficial synergistic interaction between the two metals. Monometallic Pd/TiO_2 provided improved activities to those of Au/TiO_2, most likely due to a better distribution of Pd with respect to Au during the grinding process. Based on these findings, the mechanochemical treatment of metal acetates can therefore offer a simple and efficient alternative route for the synthesis of highly active chloride-free catalysts.

Mechanochemical lignin-based reduction of noble metals is an innovative and novel technique which offers several attractive advantages over conventional solution-based NP syntheses. These include waste reduction and avoidance of solvents during synthesis as well as the use of a biomass-derived inexpensive reducing agent (lignin).[19] The total solvent-free bottom-up methodology has been recently tested by Moores *et al*. for four distinct noble metals: Au, Pd, Ru and Re. Lignin was found to play a key role as a reducing agent of metal salts to afford high quality and highly monodispersed metal NPs. The mechanical breakdown of lignin results in the formation of phenoxy radicals of considerable stability and the phenol groups adjacent to the methoxy groups in lignin structures can be oxidized and therefore play an important role as reducing agents. An interesting feature is that the product structure depends on the nature of the metal precursor used. For example, when metal chloride precursors of Pd and Ru are used, metal NPs were apparently detached from the lignin matrix, while the use of metal-organic precursors of the same metals produces a metal NP@lignin composite. Based on these observations, the right precursor can be selected to design a mechanochemical lignin-based reduction procedure to prepare either unsupported or lignin-supported NPs. Similar to lignin, another biopolymer such as chitosan, can also act as both stabilizing and reducing agent to synthesize bimetallic Au-Ag alloy nanoclusters.[20] Sequential reduction of the chloride precursors of Au and Ag generates Au-Ag alloy nanocystals (NCs) using a simple mortar grinding. These nanoclusters exhibited excellent synergistic catalytic activity toward the reduction of 4-nitrophenol. These results indicate the reducing possibilities of other biopolymers (e.g. biorefinery derived syrups)[21] in mechanochemical processes. Consequently, readily abundant biomass-derived reducing agents are a promising avenue to explore as *in situ* mechanochemical reducing agents of different metal precursors into NPs.[21]

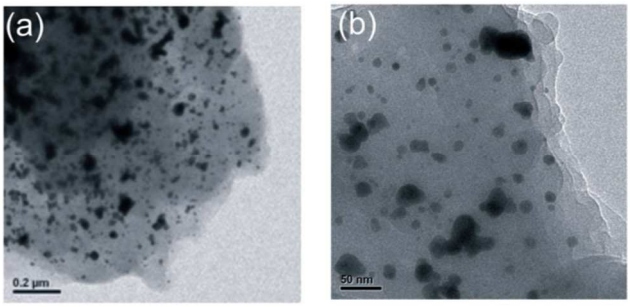

Fig 4. TEM images of mechanochemically prepared AuNP@lignin nanocomposites at different magnifications. Reproduced with permission of the Royal Society of Chemistry from reference 19.

Apart from the noble metals, dry ball milling methods can also be extended to prepare transition metal NPs (e.g. Co, Fe, Ni etc.) which are known to be conventional catalysts for the hydrogenation of CO to hydrocarbons (Fischer-Tropsch processes)[22]. Bimetallic Re-Co/Al_2O_3 catalysts can be prepared via ball milling in a shaker mill using a tungsten carbide container and tungsten carbide balls.[23] The only difference in the preparation of transition metal catalysts relates to the direct milling of metal precursors as compared to the case of noble metal NPs synthesis (in which metal salt or oxide precursors are generally used). Interestingly, mechanically prepared Re-Co containing catalysts exhibited a superior activity for methane conversion as opposed to higher rates for CO hydrogenation in catalysts prepared via incipient wetness.[23] The mechanochemically-prepared catalyst displayed a higher activity following heat treatment at 650 ºC, due to the introduction of crystallinity inside the material upon heating. Prior to heat treatment, the catalyst contained disordered Re-Co phases as indicated by powder X-ray studies. Similar to Re-Co/Al_2O_3 catalysts, Co-Fe and Ni catalysts on ZrO_2 and TiO_2 supports have also been prepared and tested for CO hydrogenation with enhanced catalytic activity.[24] Ball mill synthesized Fe NPs have shown good activity towards methane decomposition to form hydrogen.[25] Decomposition was monitored against milling time and it was observed that the amount of hydrogen generated linearly increased with milling time. SEM studies showed that the average particle size reduced with increased milling time. As a result, methane molecules were efficiently adsorbed and decomposed on newly generated iron surfaces.

Different copper based catalysts have been extensively utilised in the steam reforming of methanol (SRM) to produce high purity hydrogen for fuel cells. Mechanochemically-prepared Cu/ZnO catalysts exhibited greater stability and superior catalytic performance in SRM compared with catalysts prepared using wet-chemical methods.[26] The increased catalytic performance of mechanochemically prepared catalyst has been attributed to a greater copper dispersion and the formation of highly strained copper nanocrystals due to an enhanced Cu-Zn interaction upon mechanochemical reaction. This technique can improve the surface areas and porous structures, yielding high Cu dispersion upon reduction. An increase in surface area of Cu-ZnO catalysts could indeed be achieved if the milling process was carried out in presence of CO_2 atmosphere.[27]

During milling of copper oxides and ZnO mixtures in CO_2, the corresponding carbonates were observed as intermediates which resulted in intimate Cu–Zn mixtures upon decomposition. Recently, a planetary ball mill method has also been used for the preparation of SRM Cu/Al_2O_3 catalysts using a mixture of CuO and Al.[28] XRD and SEM revealed that the mechanochemical reaction results in the reduction of CuO to Cu(0) and the formation of amorphous alumina. Mechanochemically prepared catalysts were found to have a threefold increase in surface area (as well as reactivity) as compared to physically mixed phases.[28]

2.2 Metal oxide nanoparticles

High-energy ball milling can induce a variety of transformations in metal oxides such as amorphization, grain boundary disordering, changes in particle size and surface area and polymorphic transformations. The mechanical energy provided during grinding can also create crystal defects such as Schottky or Frenkel defects or crystallographic shear planes. Sometimes these kinds of defects can lead to interesting catalytic properties. There are several examples of the mechanochemical preparation of metal oxide nanoparticle systems with enhanced catalytic applications as compared to conventional systems.

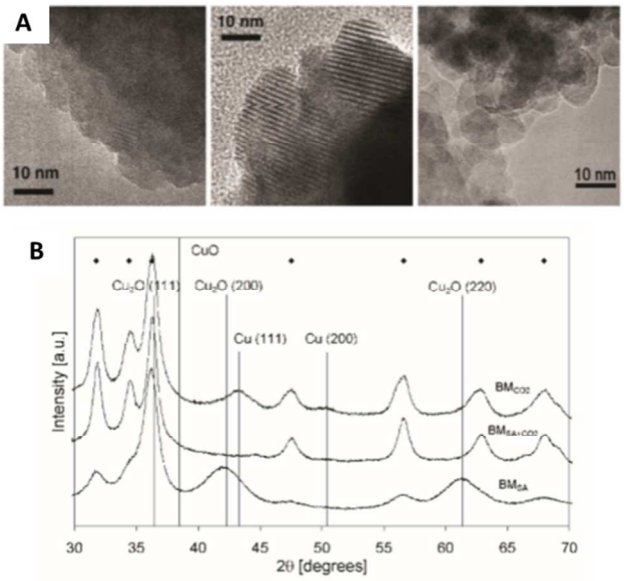

Figure 5. (A) HRTEM images of ball-milled materials. (B) XRD patterns of ball-milled materials; ZnO peaks are represented by diamonds. Reproduced with permission from Elsevier from reference 26.

Different perovskite types of catalysts have been mechanochemically prepared by the Kaliaguine group for NO_x reduction from the fundamental aspects of understanding the reaction mechanism.[29] The synthesis procedure includes a simple stepwise grinding of the mixture of required metal oxide precursors. For instance, Cu and Pd substituted Fe based perovskites could be prepared by grinding a mixture of La_2O_3, Fe_2O_3, CuO and PdO. Any additive can be easily introduced by a subsequent mechanical treatment. Cu or Pd-containing catalysts exhibited a comparatively higher activity to those in the absence of metal. This increased catalytic activity could be attributed to a

positive charge deficiency as a result of substituting Cu with the lattice Fe cation with copper cations. Similarly, the incorporation of Pd into the lattice was found to increase the catalytic activity by improving the mobility of lattice oxygen. Copper-promoted $LaCoO_3$ and $LaMnO_3$ perovskites with particle sizes between 10-20 nm were also mechanochemically prepared and investigated for the catalytic reduction of NO using propene. Both catalysts demonstrated high catalytic activity. Recently, other mixed oxide catalysts (V_2O_5/TiO_2) were also prepared for NO_x reduction under dry ball milling conditions using V_2O_5 and TiO_2 anatase, which also exhibited comparable or improved activity with respect to catalysts prepared by conventional wet impregnation methods.[30] Importantly, an increased dispersion could be achieved by increasing milling time as well as catalyst reducibility after increasing the ratio of $(V^{4+} + V^{3+})/V^{5+}$, which was correlated to the increased SCR activity.[30]

Contradictory results for mechanochemical catalysts have been also reported in literature as illustrated in the case of mechanochemically prepared catalysts with different compositions for water gas shift (WGS) reactions. Two different approaches (mechanochemical and co-precipitation) were considered to prepare a mixed rare earth oxide support.[31] Ceria supports were prepared by milling cerium hydroxide with another rare earth oxide, La, Sm, Gd or Y, followed by calcination and ultrasonic treatment. Gold was then deposited by a conventional deposition-precipitation method (Fig. 6). The synthesized catalysts were less active, less selective and less stable as compared to co-precipitation catalysts. Mechanochemically prepared catalysts have modified surfaces and larger amounts of rare earth metals on the surface can potentially influence the interaction between gold and ceria, which may account for the observed reduced catalytic activity. An alternative explanation could be the presence of surface carbonate species. The corresponding lanthanide oxide was found to be present on the surface of mechanochemically prepared catalysts which accumulates these carbonate species leading to the poisoning of active sites and thereby reducing its catalytic activity.

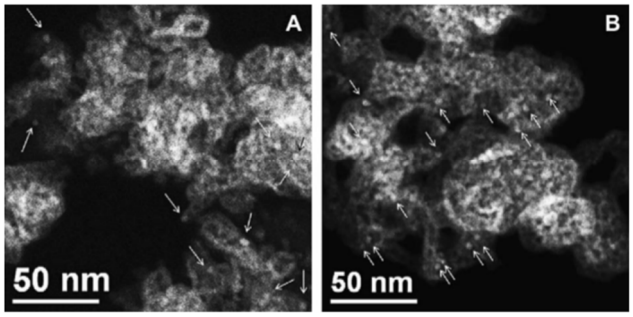

Fig. 6. HAADF images of the Au-CeY co-precipitation catalyst: (A) fresh and (B) spent. Reproduced by permission from reference 31.

In another study, ceria doped transition metal oxide catalysts FeO_x, MnO_x and CoO_x were prepared by both grinding and co-precipitation method followed by deposition of the gold, where mechanochemically ground catalysts showed comparably superior activity in WGS for these particular types of catalysts.[32] The main structural difference between these two set of catalysts was that intimately mixed oxide phases were distinctly present in the case of mechanochemically prepared materials whereas no separate phases were found using the co-precipitation method.

Similarly, mechanochemically prepared Au-Ce/Al_2O_3 catalysts using a different set of experiments demonstrated higher activity as compared to catalysts prepared by co-precipitation method.[33] Raman and Temperature Programmed Reduction (TPR) studies showed that co-precipitation catalysts contained more oxygen vacancies with respect to mechanochemical catalysts, but the oxygen vacancies were predominantly located in the bulk of the materials, unavailable for oxidation. In contrast, mechanochemically prepared catalysts were found to contain more surface oxygen vacancies available for CO oxidation. On the basis of above discussion and the differences between similar nanomaterials, the structural features of both catalysts and supports are key influential factors to control to fine-tune the catalytic activity of materials depending on their preparation methods.

Transition metal spinel oxides are widely utilised as effective catalysts for a number of industrial processes including the removal of gaseous pollutants,[34] steam/dry reforming,[35] oxidation of various compounds[36] and water-gas shift reactions.[37] The physical and catalytic properties of spinel oxides have been reported to be influenced not only by the nature and the oxidative state of the transition metal ions but also by their distribution in the spinel structure. In this regard, Manova *et al*. reported the mechanochemical synthesis of iron–cobalt spinel oxide NPs, $Co_xFe_{3-x}O_4$ (x = 1, 2), prepared by the combination of chemical precipitation with simultaneous ultrasonic treatment and subsequent mechanical milling.[38] Phase composition and structural properties of the samples were investigated by X-ray diffraction and Mössbauer spectroscopy. Prepared catalysts with different Fe/Co ratios were tested for methanol decomposition and the activities were compared with the catalysts prepared by thermal method. It was observed that the preparation method had a strong impact on the differences in the phase composition, reduction ability and catalytic behavior in methanol decomposition. In a recent report, the effect of the catalyst preparation method on methanol decomposition to CO and H_2 was described.[39] Two series of nanosized $Cu_{0.5}Co_{0.5}Fe_2O_4$ ferrites were synthesized by thermal or mechanochemical treatment of hydroxide carbonate precursor. The mechanochemical synthesis involved milling of the precursor obtained by co-precipitation in a hardened steel vessel of a planetary mill for 1–5 h. Both catalysts were found to contain an identical composition. However, XRD studies revealed that the mechanochemically prepared catalysts contained more finely dispersed ferrites and a smaller average crystallite size of 7–11 nm. Both catalysts demonstrated an almost equal activity in methanol decomposition. These results, similar to previous reports from WGS catalysts[31] clearly indicate that mechanochemistry is not necessarily the optimum/ideal technology to design advanced nanomaterials for catalytic applications which require a fundamental understanding of the mechanism and nature of the chemical process to be effectively coupled with an appropriate catalyst/support design, synthesis and optimization.

Mechanochemical grinding has also been successfully applied to prepare photocatalytic oxide NPs, towards the development of

advanced photoactive materials, Titania-based materials have been most commonly reported to be optimum photocatalysts for a wide range or processes.[40] Plesch *et al*. has reported some interesting findings on mechanochemically prepared photoactive anatase TiO_2 nanocrystals.[41] TiO_2 NCs were prepared by high energy ball milling after 3 min using $TiOSO_4{\cdot}xH_2O$ and Na_2CO_3. Photocatalytic activity is generally dependent on the morphology and crystallite size of a material. In this case, the particle size was found to directly affect the photocatalytic activity of the resulting powders. At lower temperatures (300-400 ºC), materials formed in smaller crystallite size and resulted in a decrease interfacial charge transfer due to surface charge recombination, and hence showed a reduced photocatalytic activity. On the other hand, annealing the samples above 600 ºC provided materials with equiaxial crystal length and a crystallite size between 20–40 nm. These catalysts showed relatively higher activities. Additional interesting feature in this work was the effect of milling medium in determining the properties of the catalyst. For example, the catalyst prepared in corundum jars with pure anatase phase and a crystallite size of 37 nm was found to exhibit the highest activity (doubling that of commercial P25 Evonik powder). In contrast, catalysts milled in a steel jar contained traces of rutile as well as the main anatase phase. In this case, incorporation of traces of Fe^{3+} into TiO_2 was observed which is known to catalyze the phase transformation. With these observations, the mechanochemical synthesis of Fe_2O_3/TiO_2 photocatalysts rendered photoactive materials with an activity 3–5 times greater than that of P25 Evonik. The catalysts were synthesized by milling TiO_2 and Fe_2O_3 in a planetary ball mill with a small amount of water, followed by drying.

Recently, nitrogen-doped TiO_2 materials have received much attention to achieve high photocatalytic activity with tunable energy band gaps. Various sol-gel wet impregnation and hydrothermal methods have been already established for N-doping. As compared to these traditional long methods, ball milling method allows a simple mixing of TiO_2 with nitrogen-containing materials in dry conditions. To illustrate this concept, the mechanochemical synthesis of N-doped TiO_2 catalysts for the visible liquid photocatalytic destruction of NO_x was disclosed.[42] Catalysts were prepared via high energy ball milling (100–700 rpm) of P25 TiO_2 with hexamethylenetetramine or ammonium carbonate as nitrogen sources followed by calcination at the desired temperature. During milling, both nitrogen sources decompose and release ammonia which adsorbs on the fresh TiO_2 surfaces generated by ball milling, leading to the formation of N-doped TiO_2. Similarly, many N-doped TiO_2 materials have been prepared by mechanochemistry, where different nitrogen sources were used including aqueous NH_3, NH_4F, NH_4HCO_3, NH_4COOCH_3 and urea.[43] The most interesting fact related to a strongly dependent catalytic activity with milling time and calcination temperature. Prolonged ball milling often decreased the photocatalytic activity which could be attributed to increasing the number of defects on milling as well as an observed amorphisation of the crystalline phase in titania. Furthermore, high temperature milling can promote a phase transformation from the active phase (anatase) to rutile (less active) as well as agglomeration of oxide nanoparticles, also resulting in a lower photocatalytic activity.

Other than nitrogen, mechanochemically prepared carbon-, sulfur-, and fluorine-doped TiO_2 have also been reported to exhibited increased photocatalytic activities. Yin *et al*. reported nitrogen and/or carbon doped titania photocatalysts $TiO_{2-x}A_y$ (A = N, C) prepared using a high-energy ball milling of P25 titania with different nitrogen/carbon sources including hexamethylenetetramine, admantane or ammonium carbonate, followed by calcination in air at 400 ºC.[44] A phase transformation of anatase to rutile was observed during the milling as a result of the applied high mechanical energy. Commonly, anatase is the most active photocatalytic phase of titania but there are reports of photocatalysts featuring nanosized rutile particles with large specific surface area prepared by low temperature dissolution-reprecipitation process shows higher photocatalytic activity than anatase particles.[45] The most plausible reason for such unusual behavior may relate to a smaller band gap of rutile phase (3.0 eV) which results in better absorption of visible light. The mechanochemically prepared rutile nanomaterials exhibited an excellent photocatalytic ability for nitrogen monoxide oxidation under visible light irradiation. In a similar manner, sulfur can be incorporated into TiO_2 by grinding a mixture of sulfur and TiO_2, followed by calcinations of the ground sample at 673 K in an inert gas flow.[46] The high energy ball mill produces a visible-light active $TiO_{2-x}S_x$ in rutile structure.

Wang *et al*. also synthesized fluorine-doped $SrTiO_3$ powders by a simple mechanochemical solid state reaction using $SrCO_3$ and TiO_2 in stoichiometric ratio at 1100 ºC.[47] Different fluorine sources including polytetrafluoroethylene (PTFE), SrF_2 and LiF were used in the subsequent step to get F-doped samples. Fluorine doping promoted a red shift in the absorption edge of $SrTiO_3$ and narrowed its band gap. The photocatalytic activities of both $SrTiO_3$ and F-doped $SrTiO_3$ were tested in the oxidative decomposition of NO under visible light ($\lambda > 400$ nm) and near ultraviolet light ($\lambda > 290$ nm) irradiation. F-doped $SrTiO_3$ showed three times greater activity as compared to undoped $SrTiO_3$.[47]

In addition to doping, TiO_2 can be organically functionalized by means of a reactive ball milling process. Recently, a new method has been established for the synthesis of phenylphosphonic acid functionalized titania particles using a high energy planetary ball mill.[48] This method could provide a simple and advanced route for the preparation and *in situ* surface functionalization of inorganic NPs for a wide range of catalysis applications.

ZnO-type materials are also among most commonly used photocatalysts. ZnO catalysts, prepared by milling zinc oxide and oxalic acid in an agate mill followed by thermal decomposition, showed a remarkable activity in the photocatalytic degradation of resorcinol in water.[49] Higher calcination temperature increased the crystallite size due to agglomeration, thereby reducing the photocatalytic activity. More recently, ZnO nanocrystals synthesized after reactive milling of zinc precursors with various polysaccharides as sacrificial templates including biomass-extracted agar from macroalgal species were proved to predate the photocatalytic activity of commercial P25 Evonik in the aqueous photodegradation of phenol (52 vs 30%, Fig. 7).[50]

Furthermore, the versatility of such ZnO nanomaterials was also proved as part of Poly Ether-Ether-Ketone (PEEK) nanocomposites with enhanced antibacterial activity against *Escherichia coli* and *Staphylococcus aureus* (optimum 7.5 wt% ZnO content).[51]

Improved photocatalytic activities have also been achieved by introducing a second oxide counterpart in combination with ZnO (e.g. SnO_2). For example, mechanochemically prepared SnO_2-ZnO photocatalysts exhibited enhanced photochemical activity as compared with single phase SnO_2 and ZnO.[52] The combined catalyst shows approximately 14 times higher activity than SnO_2 and three times higher to that of ZnO. The most plausible explanation for such increase in photocatalytic activity may be related to the higher specific surface area and enhanced charge separation associated with the two oxides in contact.

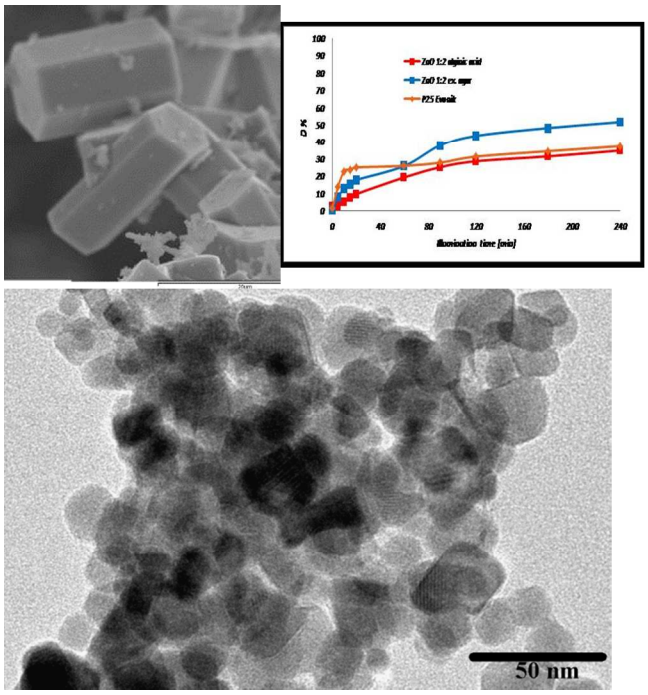

Fig. 7. Bio-templated ZnO nanocrystals as highly active photocatalysts with antibacterial properties.[50, 51] Reproduced with permission of the Royal Society of Chemistry.

Nitrogen or gallium doping of ZnO materials can render p-type ZnO materials with potentially enhanced photocatalytic properties. Many methods including pulsed laser deposition,[53] molecular beam epitaxy[54] and metal oxide chemical vapor deposition[55] are already known to make nitrogen-doped ZnO. Mechanochemical grinding can provide a simple route to obtain nitrogen-doped ZnO fine particles.[56] A serial operation of co-grinding a mixture of ZnO and urea, followed by calcination of final product at 400 ºC gives N-doped ZnO (Fig. 8). The prepared material exhibits light absorbance in the visible light wavelength region, with high photo-catalytic ability and anti-bacterial properties.

2.3 Supported nanoparticles and composite nanomaterials

Mesoporous silicas featuring high surface areas, narrow pore size distribution and tuneable pores diameters have attracted a great deal of attention in recent years due to their promising properties and applications in various areas including adsorption, separation, drug delivery, sensing and catalysis.[57] These materials can be easily modified using different methodologies (including *in situ* and post-synthetic strategies) to introduce various chemical functionalities.[57]

In recent few years, our group has extensively worked on the design of novel porous nanocomposites with different functionalities for catalytic applications. In our very first reports,[58] we devised a novel dry milling-assisted strategy for the synthesis of supported transition metal oxide nanoparticles (*e.g.*, Fe, Co, Pd) on mesoporous aluminosilicates (*e.g.*, Al-SBA-15, with a ratio of Si/Al=15). Iron oxide NPs were initially targeted in this work because of their excelling catalytic properties in a range of catalytic processes including oxidations, acid-catalysed reactions and coupling chemistries.[58]

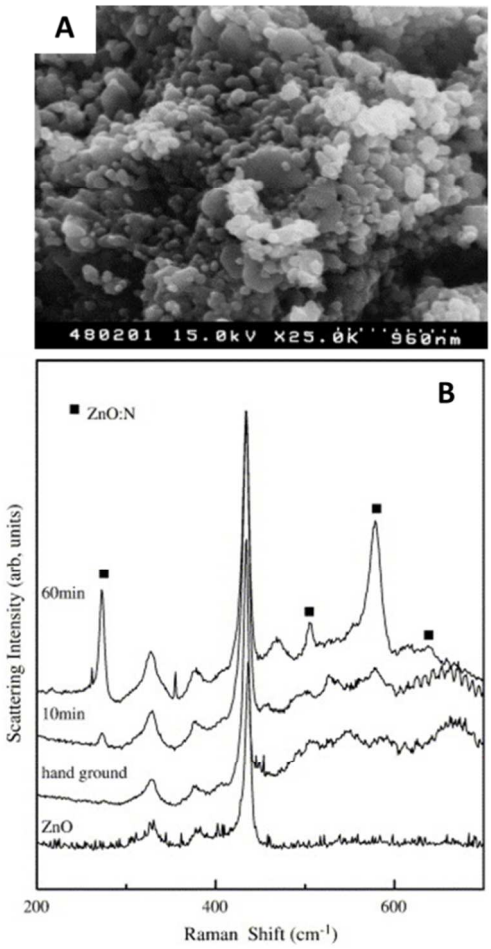

Fig. 8. (A) SEM photograph of the final calcined sample after grinding the mixture of ZnO and 5% urea for 1 h. (B) Raman spectra of material calcined at 400 °C after grinding a mixture of ZnO and 5% urea for different times.

We investigated various parameters in the synthesis of the nanomaterials including the milling speed (100 to 650 rpm) and different treatments conditions (water, formic acid and hydrogen peroxide washing under microwave irradiation) to further demonstrate that a mechanochemical process with formation of

metal oxide NPs (Fe_2O_3, NiO, etc.) occurred on Al-SBA-15 materials. The facile and efficient one-step mechanochemical approach produced highly active and well-dispersed NPs with highly preserved structures and textural properties (XRD patterns, high surface areas, pore sizes, and volumes) under optimum conditions (dry milling, 350 rpm, 10 min). An incipient deterioration was comparatively observed for materials milled at 650 rpm clearly pointed out by the presence of amorphous silica domains in TEM micrographs of high speed ball-milled materials (Fig. 9). The catalytic activity of the synthesized materials was investigated in the microwave-assisted oxidation of benzyl alcohol and the alkylation of toluene using benzyl alcohols. Comparable and even higher catalytic activities were observed even at very low iron loading (as low as 0.08 wt.%) for the mechanochemical materials (ca. 50-55% conversion for both the microwave-assisted oxidation of benzyl alcohol and alkylation of toluene with benzyl chloride) with respect to catalysts prepared using a conventional impregnation method containing ten times more iron (ca. 0.7 wt.% Fe, 35-40% maximum conversion under identical reaction conditions).[58a]

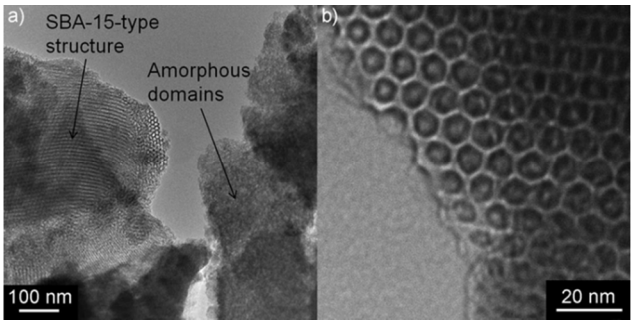

Fig. 9 TEM micrographs of 350Fe/Al-SBA-15-HP. The images clearly depict (a) an amorphous silica domain (right hand side) as compared to (b) a hexagonal SBA-15-type structure. Copyright by Wiley VCH-Verlag. Reproduced with permission from reference 58a.

A subsequent extension of this catalytic system comprised the hydroarylation reaction of phenylacetylene to 1,1-diarylalkenes under microwave irradiation (Scheme 2). Fe/Al-SBA-15 catalysts were proved to be highly active and selective to yield substituted alkenes in short reaction times and were reusable under the investigating conditions, preserving almost 90% of its initial activity after three consecutive runs.

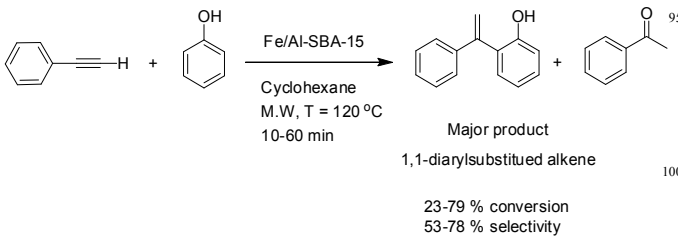

Scheme 2.Hydroarylation of phenylacetylene with phenol/s catalyzed by supported iron oxide nanoparticles on aluminosilicate materials under microwave irradiation.

The versatility of the proposed mechanochemical catalysts was further expanded to hydrogenation and hydrogenolysis of lignin using a similarly synthesized metal-based aluminosilicate SBA-15 nanocatalysts.[59, 60] A series of hydrogen-donating solvents including tetralin, isopropanol, glycerol and formic acid were utilised as hydrogen sources for *in situ* hydrogen generation under heating in the presence of the catalyst. Studies on different metals and metal contents including nickel (2, 5 and 10 wt.%), palladium (2 wt.%), platinum (2 wt.%) and ruthenium (2 wt.%) proved that depolymerization of lignin could be effectively catalyzed by 10 wt.% Ni was found to achieve the highest lignin depolymerization degree, with a maximum yield of 35% bio-oil production containing simple aromatics (syringaldehyde, vanillin, aspidinol, etc.) under mild hydrogen-free microwave irradiation conditions.[59, 60]

Further exploration of mechanochemical processes with iron oxides based on fundamental understanding of catalyst preparation and design as well as the remarkable advantages of mechanochemistry in catalyst development led to the preparation of advanced catalytic SBA-15/maghemite nanocomposites featuring magnetic separation.[61] Magnetically separable nanocomposites (MAGSNCs) are of special interest, offering a promising magnetic separation feature that can meet the requirements of high activity and accessibility to active sites with improved reusability.[62] MAGSNCs can also offer important advantages in a wide range of catalyzed reactions due to their potential for further functionalization with controllable surface functionalities.[63]

These advanced nanomaterials were synthesized using an unprecedented one-pot mechanochemical solvent-free dry milling approach (Scheme 3). In this way, Pd-containing MAGSNC materials could be prepared by simply grinding together solid $Fe(NO_3)_3{\cdot}9H_2O$, an appropriate quantity of propionic acid (as reducing agent to form the maghemite phase), Pd acetate (or any solid metal precursor i.e. $NiCl_2$, $RuCl_3$, etc.) along with solid SBA-15 silica support under mild reaction conditions (350 rpm, 10 min) in a planetary ball mill.[61b] Functionalisation was found to be possible with noble or transition metals (*e.g.*, Ru, Ir, Ag, Ni, Cu, Co, etc.) as well as with other types of functionalities using the proposed protocol. The functionalized Pd-MAGSNC nanocatalysts demonstrated high activity towards aqueous Suzuki coupling reactions at room temperature and most importantly the magnetic susceptibility of the maghemite phase was preserved even after several catalytic runs, which confirmed the stability of the mechanochemically synthesized nanocomposites under the investigated reaction conditions.[61]

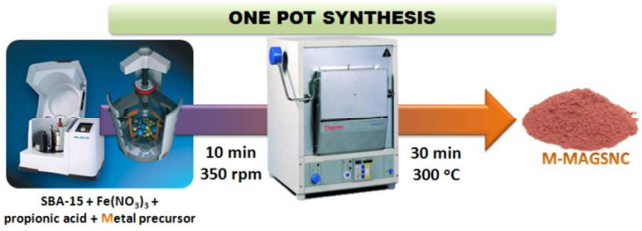

Scheme 3. Overview of the preparation of functionalized magnetic nanocomposites.

Similarly, the design of novel Cu-containing aluminosilicate catalysts on the basis of ball mill synthesis was conducted and synthesized materials tested in the microwave-assisted aqueous conversion of glucose to valuable reduced products.[64] Formic acid served as both dehydration co-catalyst and

hydrogen-donating solvent. The combined catalytic system offered a simple one-pot route for glucose conversion *via* tandem formic acid-promoted dehydration to 5-hydroxymethylfurfural (HMF) and further selective hydrogenation to 5-methylfurfuryl alcohol (MFA). Two types of aluminosilicate materials with and without Zn in their composition along with active Cu NPs were tested. A Zn-synergetic effect was observed in CuAlZn–SBA as compared to CuAl–SBA in terms of selectivity to advanced hydrogenated products (e.g. MTHFA, Fig. 10). Zn was found to play an interesting role in the selectivity to reduced products, even in very small quantities (0.2 wt%). The present technique represents a unique and unprecedented protocol that may pave the way to future studies on related tandem chemistries (*e.g.*, dehydration/oxidation; dehydration/esterification as well as C–C and C–O couplings) to a wide range of high value added products from sugars (Scheme 4).[65]

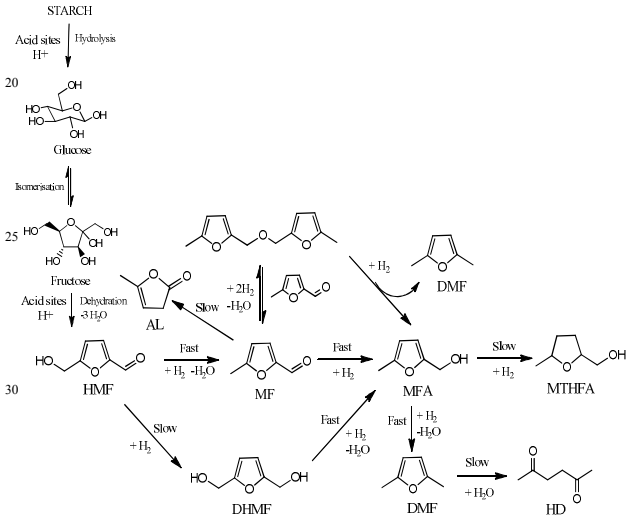

Scheme 4. Pathways and steps for the conversion of starch-derived materials into valuable furanics. Adapted from Reference 65. Reproduced by permission of the Royal Society of Chemistry.

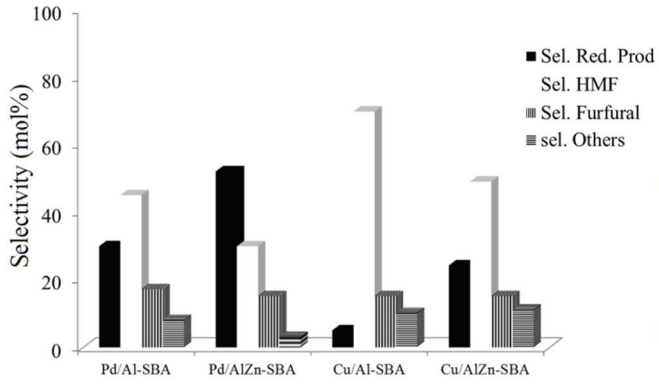

Fig. 10. Changes in Selectivity (Y axis, mol%) for the production of HMF (white bars) vs selectivity to reduced products (sel. red. prod., black bars) of various metal/AlZn-SBA catalytic systems in the microwave-assisted conversion of starch. Reaction conditions: 0.05 g starch, 0.5 mL H_2O, 0.5 mL formic acid, 0.02 g catalyst, microwaves, 300 W (maximum temperature reached 183ºC, average temperature 181ºC), 5 min. reaction time.

Zeolites are widely utilised materials in several catalytic applications. However, traditional synthesis methods comprise rigorous and long workup steps along with the drainage of bulk amount of solvents. The search for new and improved methods to synthesize and modify zeolites remains a central topic of academic and industrial relevance. Solvent-based methods have several drawbacks including the need for subsequent workup steps and the huge amount of liquid waste. Mechanochemistry has been postulated as a scalable, one-step approach to overcome these limitations for zeolite synthesis. Very recently, mechanochemical reactions for zeolites syntheses and their use in catalysis have been summarized in an excellent overview by Perez-Ramirez *et al*., where structural features of such zeolites have been critically discussed in detail.[66]

Mechanochemistry opened such innovative possibilities to construct zeolite-type catalysts with improved catalytic activities by exposing additional active sites and increasing external surface areas. Along with determining particle size and surface area, milling can also affect the strength and number of acidic and basic sites in zeolites.[67] New weak Lewis acid sites can sometimes be generated during the milling process.[67] Enhanced selectivity in zeolite (*e.g.* KNa-X zeolites) can be achieved by tuning the amount of Lewis acid and basic sites.[68] Balaz *et al*. have reported the advantages of a mechanically prepared Mo-containing beta-zeolite catalyst compared with an impregnated analogue in the hydrodesulfurization of thiophene, where the pore size and surface area were found to vary depending on the preparation method.[69] Mechanically treated materials contained larger pores and smaller surface areas as compared to impregnated materials. The accumulated energy provided during the milling helps in the spontaneous surface reconstruction of the catalyst which was claimed to account for the observed superior catalytic activity.

Titanium-containing zeolites (titanosilicates, TS) are of great importance due to their remarkable catalytic activities in various oxidation reactions.[70] Under traditional hydrothermal synthesis, a Ti source (any titanium alkoxides such as tetrabutyl orthotitanate) is co-polymerized with a silicon alkoxide to form a precursor hydrogel. Upon subsequent hydrothermal treatment, Ti species are introduced in the amorphous silica matrix. The tetrahedrally-coordinated Ti atoms substitute isostructural Si atoms in the zeolite framework, generating the catalytically active sites in TS. However, due to the differences in the hydrolysis rates of titanium and silicon alkoxides, titanium alkoxides are often aggregated separately to form octahedral Ti species, which are catalytically inactive for oxidation reactions. This serious problem can be circumvented under a direct synthetic protocol that avoids polymerization of monomer precursors.

Yamamoto *et al*. described the synthesis of titanosilicate TS-1 catalysts from inexpensive precursors (titania and silica) using a planetary ball mill.[71] In contrast to conventional methods, the proposed approach avoids the use of expensive titanium alkoxide reagents as Ti source which is indeed a great advantage in large scale synthesis. Ti atoms in the bulk titania were dispersed into the amorphous silica matrix via mechanical grinding to form an uniform silica–titania composite. The prepared precursor nanocomposite was then crystallized into TS-1 by subsequent hydrothermal treatment in the presence of a typical

structure-directing agent (e.g. tetrapropylammonium hydroxide). The activity of the resulting materials was investigated in the oxidation of 1-hexene using hydrogen peroxide. Comparable activities were obtained for both mechanochemically and conventionally prepared catalysts. However, it was observed that grinding time had a significant impact on the catalytic activity. Longer grinding times (i.e. over 12 h) were found to promote the mechanochemical reaction and produced exclusively tetrahedral Ti sites, which demonstrated good catalytic activity. Comparably, octahedral Ti sites could be observed at shorter grinding times (3 h) which influenced the catalytic activity of the material since octahedral Ti sites are unable to act as active catalytic centers. As expected, prolonged grinding times (24–48 h) had a detrimental effect on the activity despite the presence of only tetrahedral Ti species due to an increased contamination with zirconium, present in the grinding medium. Zr atoms compete with Ti for incorporation into the framework of the material and therefore reduce the surface hydrophobicity as well as the presence of Ti framework sites.

The other factor which generally influences the catalytic activity is the rotation speed. For example, low rotation speeds cannot often produce enough energy to remove the octahedral sites and generate the desired tetrahedral sites, while higher rotation speed result in the desired tetrahedral sites. However, the resulting materials also contained more zirconium at higher rpm. Despite the contamination found under milling conditions, zirconia ceramics provided optimum results as grinding media. Higher density balls increase the impact energy under ball milling which is important to promote the mechanochemical reactions.

Recently, Iwasaki *et al*. described a mechanochemical route for an alkoxide-free synthesis of TS-1 powder with high catalytic activity using inexpensive materials in a planetary ball mill at a low rotational speed (140 rpm).[72] A low-grade amorphous fumed silica and crystalline anatase-type titania nanoparticles were mechanochemically treated under dry conditions using a tumbling ball mill to form the silica–titania nanocomposite precursors. Similar to the previous example, this precursor was then hydrothermally treated with tetrapropylammonium bromide (TPABr) and *n*-butylamine (NBA) as structure-directing agent to facilitate the crystallization. Morphologically, the material consisted of coffin-shaped particles in the size range 5–10 μm (Fig. 11). Impressively, the material cost of this mechanochemical method was less than 5% of those prepared using conventional sol-gel methods.[72]

Porous nanocomposites of thin hydrophobic carbon layers and nanosized metal oxide particles have great importance for their high efficiency in catalysis and specific adsorption under moisture conditions. Graphite is one of the most suitable form of carbon supports in this purpose because of its high specific surface area and presence of huge number of open sites for functionalization. Graphite oxide (GO) shows a rich intercalation chemistry owing to its excellent swelling and related properties, similar to clay minerals.[73]

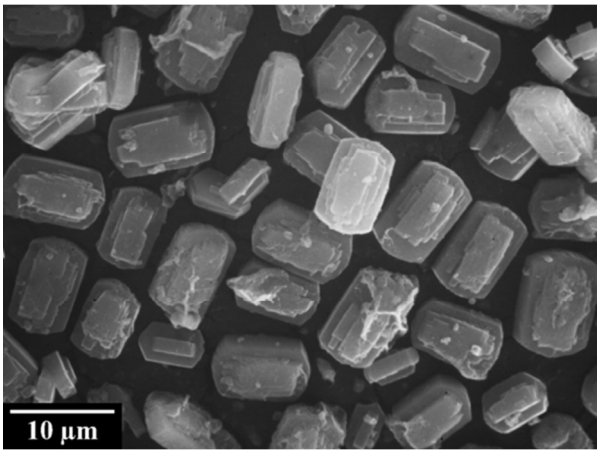

Fig. 11 SEM image of mechanochemically prepared TS-1 particles.

Mechanochemical methods can be a simple but very effective means to improve tetraethoxylsilane (TEOS) intercalation reaction into layer materials. In a recent report, the concept of mechanochemical intercalation was applied to introduce controlled amount of TEOS into surfactant-preexpanded GO.[74] Small amount of added TEOS produced a more expanded ordered layer structure with the interlayer distance, while large amounts of added TEOS induced layer delamination, resulting in a less ordered structure. Up to a particular limit, the porosity of the calcined composites was shown to increase with the increase of silicon content after which dramatically decreased with the increase of TEOS addition. These findings indicate the important role of the composition state of silica particles and carbon layers in the formation of porosities. Fig. 12 demonstrates the typical intercalation and porosity formation mechanism in TEOS/GO materials as a result of mechanical treatment. Firstly, the long-range layered structure of GO is expanded via surfactant intercalation to arrange the surfactant molecules in an inclined direction or by pseudo-trilayer stacking.

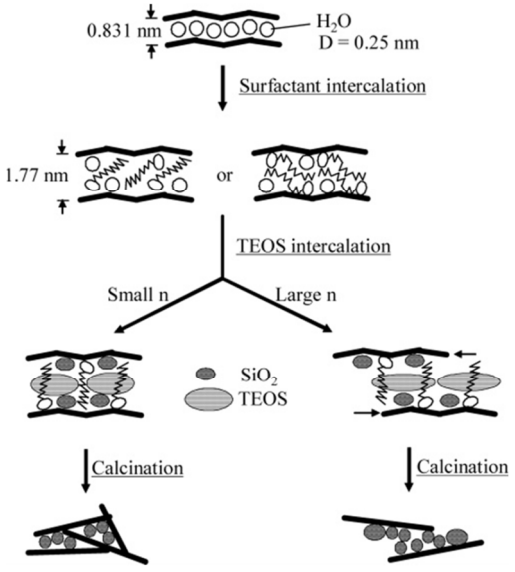

Fig. 12 Schematic representation of intercalation and pore formation mechanisms in TEOS/GO nanocomposites.[74]

Surfactant molecules replace about 55% of ion-exchange sites, leaving the other 45% of ion-exchange sites retained in GO layers which form a microscopic hydrophilic environment among the surfactant-modified hydrophobic GO interlayers (and can provide sites for TEOS hydrolysis). The intercalation of TEOS is initiated under milling-induced interaction of TEOS with surfactant-pre-expanded GO samples to form an expanded regularly layered structure. The driving force comes from the hydrophobic attraction in the interlayer.

Another example of mechanochemical synthesis of metal oxide doped graphene has been recently reported by Li *et al*.[75] A one-step, low-cost, and up-scalable *in situ* wet-mechanochemical method was used to synthesize SnO_2@graphene nanocomposites. Graphene oxide and $SnCl_2$ were used as precursors. Graphene oxides were reduced to graphene while $SnCl_2$ was oxidized to SnO_2 nanoparticles that were *in situ* anchored onto the graphene sheets, resulting in uniform and resilient nanocomposites. The present method provides a highly promising alternative to conventional methods for GO nanocomposite preparation as well as a potential further extension for the large-scale production of a series of metal oxides@graphene composites or other materials for practical applications in catalysis, energy storage and different other fields.

The mechanochemical synthesis of cystine-capped CdSe@ZnS nanocomposites was also recently reported to provide possibilities for nanomaterials with promising uses in biomedicine for biosensing applications.[76] Synthesized CdSe@ZnS nanocomposites were capped with L-cysteine which underwent oxidative coupling to form cystine (with a covalent disulphide bond between the two cysteine R groups) during the milling process. The stability and unique capping of CdSe@ZnS nanocomposites with cystine was proven by FTIR spectroscopy and found to be related to the presence of water molecules in the systems, in good agreement with other reports[58, 61], where CdSe@ZnS particles acted as catalyst to promote the aforementioned oxidative coupling. Such unprecedented capping prevented the leaching of toxic cadmium ions into physiological solutions, potentially providing an interesting type of nanomaterials with improved biocompatibility.

High energy ball milling processes can also be efficiently used in the conversion of carbon allotropes. For instance, a recent report demonstrates a high-energy ball milling technique for large-scale synthesis of nitrogen doped carbon nanoparticles (NDCPs) from graphite.[77] High mechanical energy breaks down the strong bonds of graphite upon disruption of the layers to produce free valences along the fresh borders, which paves the way for the formation of carbon nanostructures with new functionalities. The synthesis is carried out under ball milling of pristine graphite powders in a high-energy rolling ball mill in the presence of nitrogen gas (300 kPa) at room temperature. In the subsequent step, the milled samples are heated in a horizontal tube furnace from room temperature to 700 ºC and then annealed in the presence of N_2–15% H_2 mixture gas. NDCPs materials exhibited a high performance as electro-catalysts for oxygen reduction reactions which could potentially replace well known and currently extended Pt-based materials. The materials also exhibited an excellent tolerance to methanol in comparison to other non-precious metal catalysts. The synthetic strategy demonstrated a general low-cost approach to fabricate novel carbon-based structures which can be potentially easy to scale up, providing a feasible method for the development of large-scale practical electrocatalysts.

2.4 Metal-organic and covalent organic frameworks

Metal-organic frameworks (MOFs) represent a new class of hybrid organic-inorganic supramolecular materials comprising ordered networks formed from organic electron donor linkers and metal cations.[78] MOFs feature large surface areas, tunable pore sizes and functionalities and can act as hosts for a variety of guest molecules. Due to these excellent physicochemical properties, MOFs are now widely explored for a range of applications in gas separation, catalysis, drug delivery, optical and electronic applications, and sensing.[78, 79] Several examples of MOF-based catalytic processes have been summarized in some already published excellent reviews.[80, 81] Considerable efforts have been devoted to the synthesis of MOF materials. Most synthetic processes of MOFs are generally carried out in the liquid phase, either using pure solvents or a suitable solvents mixture. Typical MOF syntheses involve heating a mixture of ligands and metal salts under solvent reflux for 12–48 h. Although these procedures can yield high quality crystals, the protocols require a long time of reaction, a significant energy and resource input, with most processes being unable to be scale-up from gram/multi-gram scale. Improvements in this area are consequently needed for both scale up purposes and to reduce synthesis time and milder reaction conditions. Solvent-free ball milling or liquid-assisted grinding (LAG) emerged as promising alternatives for MOF synthesis.

The first mechanochemical synthesis of MOF was reported in 2006 by Pichon *et al*.[82] where simple grinding of copper acetate and isonicotinic acid originated a highly crystalline and single-phase product of $[Cu(INA)_2]$ within just 10 minutes of grinding in the absence of any heating. The pores inside the material contained acetic acid and water molecules which could be removed by thermal activation to yield the guest-free porous compound.[82] The same group has extensively worked on the solvent-free mechanochemical syntheses of MOFs including systematic studies using 60 mixtures between 12 metal salts (Ni, Cu, or Zn with various counterions) and five carboxylate-based organic linker molecules.[83] Among the sixty possible combinations, 40 gave crystalline product including two porous compounds ($[Cu(INA)_2]$ and HKUST-1) and 29 reactions were quantitative.

In some cases metal salts can be replaced by metal oxides as a starting material which results in the formation of water as only side product. Solvent-free grinding can be exclusively applied in this situation due to the low solubility of metal oxides in any solvent. However in some cases, small amounts of deliberately added solvent in a LAG has been shown to have profound advantages including (i) acceleration of the mechanochemical reactions, probably due to an increase of mobility of the reactants on the molecular level, (ii) homogenization of reactants by the solvent, making the reaction well defined towards completion and (ii) structure-directing properties exerted by the solvent during the reaction. Some recent reports have demonstrated the efficient

use of ion- and liquid-assisted grinding (ILAG) process for the selective construction of pillared-layered MOFs, where both ions solvents exert a structure-directing effect.[84]

The structure, stability and reactivity of MOFs under mechanochemical reaction conditions often dramatically differ from conventional synthesis routes. A simple example can prove this fact. The structural interconversion of nonporous solvated Zn terephthalates between their three different forms was disclosed to be very labile in grinding-induced mechanochemical processes while this is not generally possible by simply immersing the same MOF in the particular solvent (Fig. 13).[85] Three different topologies (**1**, **2** and **3**) are interconvertable within minutes by grinding with small amounts of added liquid (LAG) or with additional solid ligands in the complete absence of added solvent. Simple immersion technique does not allow these interconversions (except **2** and **3** to **1** using one molecule of added H_2O).

Banerjee and coworkers reported three isoreticular covalent organic frameworks (COFs) synthesized by mechanochemical (MC) grinding and solvothermal methods.[86] Solvent-free mechanochemically synthesized COFs were shown to have improved thermal and chemical stabilities as compared to MOFs prepared via solvothermal route. MC COFs had moderate crystallinity with remarkable stability in boiling water, acid (9 N HCl) and base as well as offered the possibility to be exfoliated during the synthesis to give a graphene-like layered morphology; unlike the parent solvothermally synthesized COFs.

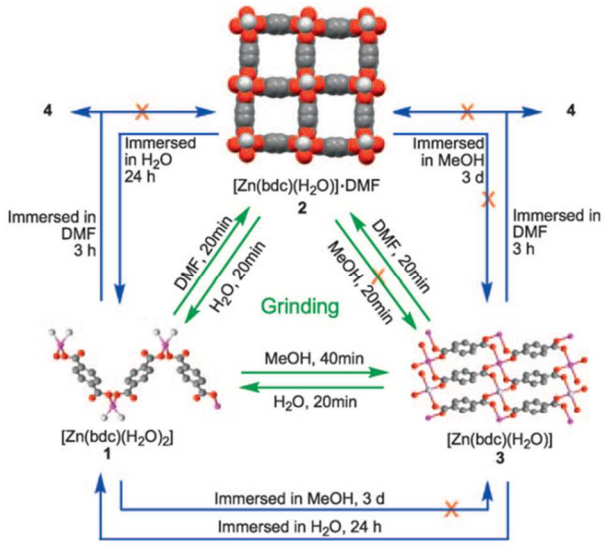

Fig. 13 Interconversions between 1, 2, and 3 induced by grinding (inner, green arrows) compared with simple immersion in excess of the liquid (outer, blue arrows).

Mechanochemically synthesized MOFs can also exhibit different catalytic activities as compared to solvothermally synthesized analogues. In a very recent report, Li *et al.*[87] introduced six-coordinated nickel clusters into a zinc-based ZIF-8 structure (designated as BIT-11) via one-pot mechanochemical synthesis under LAG conditions. Similar Ni substitution was carried out under solvothermal conditions to form BIT-11b single crystals. Interestingly BIT-11 can selectively pick different alcohol molecules according to their shapes and undergo a de-coordination to form stable four-coordinated Ni clusters BIT-11b. BIT-11 and BIT-11b possessed different applications due to the distinct coordination modes of Ni in these two frameworks.[87] The meta-stable and green colored BIT-11 comprises distorted six-coordinated Ni ions, which can easily transform into violet BIT-11b triggered by small polar solvent molecules. This transformation can be utilized to selectively and precisely sense and detect different alcohol molecules in a time-resolved manner. In contrast to BIT-11, BIT-11b synthesized under solvothermal conditions possess tetrahedrally coordinated photoactive Ni centers and open channels, exhibiting outstanding photocatalytic activities under visible light.[87]

Another recent report discloses the simple fabrication of zeolitic imidazolate frameworks (ZIFs) via mechanochemical dry milling.[88] ZnO crystals could be converted into pure phase ZIF-8 with a polycrystalline grain boundary and a core-shell structure under solvent- and salt-free conditions. These ZIF-8 polycrystals possessed higher surface areas comparable to those of conventional ZIF-8 monocrystals. As shown in Fig. 14, the polycrystallization of ZIF and inclusion of ZnO comprises three steps (1) breakage of NP agglomerates, (2) complex forming reaction between ZnO and an imidazole ligand, and (3) the nanoparticle agglomeration, resulting in the formation of a ZIF cover overlying ZnO. In spite of being in principle a solvent-free process, the water released from the reaction between ZnO and imidazole is believed to help in the formation of the complex between ZnO and imidazole ligands. Once ZIF-8 deposition and subsequent NPs agglomeration proceed to some extent, the conversion of ZnO to ZIF-8 is stopped. This method indeed has a remarkable potential for the convenient one-pot synthesis of related ZIF nanocomposites as well as the development of novel MOF-type materials from a green chemistry standpoint.

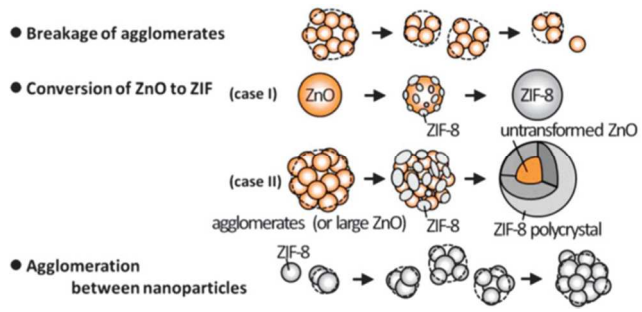

Fig. 14 Proposed mechanism for mechanochemical dry conversion of ZnO to ZIF-8. The three main processes take place in parallel.

3. Conclusions and future prospects

The proposed contribution has been aimed to provided a brief overview of key mechanochemical approaches for the synthesis of nanomaterials for diverse catalytically related applications. In addition to solvent-free synthesis of catalysts, LAG was proved to have relevant advantages as compared to dry milling protocols and conventional syntheses. Through this fascinating journey from history to synthesis and applications, the potential of

mechanochemically synthesized nanomaterials is very significant. In many cases, mechanochemical nanomaterials and nanocatalysts exhibit comparable or improved catalytic activities as compared to conventionally synthesized materials by traditional methods.

Despite the remarkable potential of mechanochemical syntheses in the effective design of advanced nanomaterials, these protocols are far from being ideal. The design of nanocatalysts needs to be based on fundamental understanding of both the application (e.g. catalysis, type of reaction, mechanism) as well as the type of material to be prepared. One of the main issues of mechanochemical processes lie in the relatively poor controllability and understanding of the systems to design tunable nanomaterials with desired properties including specific surface areas, porous structure, phase composition, crystallization degree, morphological properties, defectiveness, dispersion, structural and mechanical properties, distributions of components on the supports, etc. Many impressive examples of oustanding syntheses of valuable materials via mechanical treatment still have no clear underlying mechanism due to the nature of the milling approach (e.g. sealed, rapidly moving reaction chambers-milling jars-, rapid and violent motion of the milling media, etc.). In fact, most of current highlighted materials from this work, including own work, lack of an appropriate mechanism to show light into the mechanochemical process. Further research should be directed towards a better understanding of mechanochemical reactions at microscopic or molecular levels for its practical implementation and progress in all divisions of catalysis.

In situ and real time monitoring studies of mechanochemical transformations are recent remarkable achievements from the group of Friscic to advance in the mechanistic understanding at the molecular level.[89, 90] In these studies, authors demonstrated a remarkable possibility for in-situ determination of changes in size in milled particles, something of relevance and uniqueness for the design of nanomaterials with tunable (nano)particle sizes for specific applications (e.g. particle size-dependent catalytic reactions).[22, 91] However, only few reports have been recently disclosed which employ different techniques such as *in-situ* X-ray diffraction[89] and Raman spectroscopy.[90]

In situ diffraction of high-energy synchrotron X-rays allowed the real-time characterization and monitoring of crystalline solids without disturbing the milling process.[89] Transformations of reaction intermediates and the indirect detection of amorphous phases (*e.g.* by the disappearance of crystalline organic reactants) were also possible outputs of the proposed methodology. Some model studies have been already monitored by this technique. For instance, reaction profiles, formation of intermediates, and interconversions of framework topologies could be directly monitored in the mechanosynthesis of metal–organic frameworks which revealed that mechanochemistry is highly dynamic in terms of reaction rates (comparable to or greater to those in solution phase).

In contrast to *in situ* X-ray diffraction method, *in-situ* Raman scattering method was proved to be sensitive for crystalline, amorphous and liquid reaction participants since it enables a direct insight into the mechanochemical transformations at the molecular level.[90] The work by Sepelak *et al*. along the lines of multi-faceted studies of mechanochemically synthesized nanomaterials also combined a number of spectroscopy techniques including Mössbauer, Raman and solid-state NMR with diffraction and electron microscopy for an unique characterisation approach of mechanochemical materials.[92] Further challenges in mechanochemistry include also include improvements related to scalability, quantitativeness and greater control over reaction conditions.

On the basis of all recent outstanding findings, more improved protocols can be devised which could allow us to operate the mechanochemical reactions as per our requirements. It is now very timely to undertake such research efforts because of the growing need of mechanochemistry to develop alternative and more sustainable production methods for nanomaterials production. Further investigations are thus required and we hope that this feature article can motivate many researchers to contribute with more interesting findings in the near future to advance the knowledge in mechanosynthesis as a field of mainstream research area.

Acknowledgements

Sudipta De gratefully acknowledges University Grants Commission (UGC), India and University of Delhi for the financial support and necessary journal access for this work. Rafael Luque gratefully acknowledges funding from projects CTQ2011-28954-C02-02 (MINECO) and P10-FQM-6711 (Consejeria de Ciencia e Innovacion, Junta de Andalucía).

Notes and references

[a]*School of Food and Biological Engineering, Zhengzhou University of Light Industry, Dongfeng Road 5, Zhengzhou, Henan, 450002, P.R. China*
[b]*Laboratory of Catalysis, Department of Chemistry, University of Delhi, North Campus, Delhi-110007, India; E-mail: sudiptade22@gmail.com*
[c]*Department of Catalysis and New Chemistries, Avantium Chemicals, Zekeringstraat 29, 1014 BV, Amsterdam, The Netherlands*
[d]*Departamento de Química Orgánica, Universidad de Córdoba, Edificio Marie Curie (C-3), Ctra Nnal IV-A, Km 396, 14014 Córdoba, Spain. Fax: +34957212066; Tel: +34957212065; E-mail: q62alsor@uco.es*

1. (a) B. Rodriguez, A. Bruckmann, T. Rantanen and C. Bolm, *Adv. Synth. Catal*. 2007, **349**, 2213; (b) K. Tanaka, *Solvent-free Organic Synthesis*, Wiley-VCH, Weinheim, 2nd edn, 2008; (c) M.A.P. Martins, C.P. Frizzo, D.N. Moreira, L. Buriol and P. Machado, *Chem. Rev.* 2009, **109**, 4140.
2. G. A. Bowmaker, *Chem. Commun*. 2013, **49**, 334.
3. L. Takacs, *J. Met.* 2000, **52**, 12.
4. (a) M. Faraday, *Q. J. Sci., Lit., Arts* 1820, **8**, 374; (b) L. Takacs, *J. Therm. Anal. Calorim.* 2007, **90**, 81.
5. M. C. Lea, *Br. J. Photogr*. 1866, **13**, 84.
6. M. C. Lea, *Am. J. Sci*. 1893, **46(3)**, 413.
7. G. Heinicke, *Tribochemistry*, Akademie Verlag, Berlin, 1984.
8. J.F. Fernandez-Bertran, *Pure Appl. Chem.* 1999, **71**, 581.
9. (a) S. L. James, C. J. Adams, C. Bolm, D. Braga, P. Collier, T. Friscic, F. Grepioni, K. D. M. Harris, G. Hyett, W. Jones, A. Krebs, J. Mack, L. Maini, A. G. Orpen, I. P. Parkin, W. C. Shearouse, J. W. Steed and D. C. Waddelli, *Chem. Soc. Rev*. 2012, **41**, 413; (b) P. Balaz, M. Achimovicova, M. Balaz, P. Billik, Z. Cherkezova-Zheleva, J.M. Criado, F. Delogu, E. Dutkova, E. Gaffet, F.J. Gotor, R. Kumar, I. Mitov, T. Rojac, M. Senna, A. Streletskii, K. Wieczorek-Ciurowa, *Chem. Soc. Rev.* 2013, **42**, 7571.

10. (a) A. L. Garay, A. Pichon and S. L. James, *Chem. Soc. Rev*. 2007, **36**, 846; (b) V. Sepelak, A. Düvel, M. Wilkening, K.D. Becker, P. Heitjans, *Chem. Soc. Rev*. 2013, **42**, 7507.
11. (a) A. Pichon and S. L. James, *CrystEngComm* 2008, **10**, 1839; (b) W. Yuan, T. Friscic, D. Apperley and S. L. James, *Angew. Chem. Int. Ed*. 2010, **49**, 3916; (c) T. Friscic, *Chem. Soc. Rev*. 2012, **41**, 3493.
12. J. Huot, D. B. Ravnsbæk, J. Zhang, F. Cuevas, M. Latroche and T. R. Jensen, *Progress Mater Sci*. 2013, **58**, 30.
13. (a) B. Kubias, M. J. G. Fait and R. Schlogl, in *Handbook of Heterogeneous Catalysis*, ed. G. Ertl, H. Knozinger, F. Schüth and J. Weitkamp, Wiley-VCH, Weinheim, 2nd ed, 2008, p. 571; (b) K. Ralphs, C. Hardacre and S. L. James, *Chem. Soc. Rev*. 2013, **42**, 7701.
14. (a) U. Kamolphop, S. F. R. Taylor, J. P. Breen, R. Burch, J. J. Delgado, S. Chansai, C. Hardacre, S. Hengrasmee and S. L. James, *ACS Catal*. 2011, **1**, 1257; (b) K. Ralphs, C. D'Agostino, R. Burch, S. Chansai, L. F. Gladden, C. Hardacre, S. L. James, J. Mitchell and S. F. R. Taylor, *Catal. Sci. Technol*. 2014, **4**, 531.
15. Y. Lin, K. A. Watson, M. J. Fallbach, S. Ghose, J. G. Smith, D. M. Delozier, W. Cao, R. E. Crooks and J. W. Connell, *ACS Nano* 2009, **3**, 871.
16. A. R. Siamaki, Y. Lin, K. Woodberry, J. W. Connell and B. F. Gupton, *J. Mater. Chem. A* 2013, **1**, 12909.
17. M. J. Rak, N. K. Saadé, T. Friščić and A. Moores, *Green Chem*. 2014, **16**, 86.
18. S. A. Kondrat, G. Shaw, S. J. Freakley, Q. He, J. Hampton, J. K. Edwards, P. J. Miedziak, T. S. E. Davies, A. F. Carley, S. H. Taylor, C. J. Kiely and G. J. Hutchings, *Chem. Sci*. 2012, **3**, 2965.
19. M. J. Rak, T. Friscic and A. Moores, *Faraday Discuss*. 2014, **170**, 155-167.
20. A. Murugadoss, N. Kai and H. Sakurai, *Nanoscale* 2012, **4**, 1280.
21. R. Luque, R. Campos, A. Garcia, C. Lastres, M. Ojeda, A. Pineda, A.A. Romero, A. Yepez, *RSC Adv*. 2013, **3**, 7119.
22. R. Luque, A.R. de la Osa, J.M. Campelo, A.A. Romero, J.L. Valverde, P. Sanchez, *Energy Environ. Sci*. 2012, **5**, 5186.
23. L. Guczi, L. Takacs, G. Stefler, Zs. Koppany and L. Borko, *Catal. Today* 2002, **77**, 237.
24. F. Delogu, G. Mulas and S. Garroni, *Appl. Catal., A* 2009, **366**, 201.
25. S. Motozuka, M. Tagaya, M. Morinaga, T. Ikoma, T. Yoshioka and J. Tanaka, *Int. J. Powder Metall*., 2012, **48**, 21.
26. L. Wang, Y. Liu, M. Chen, Y. Cao, H. He, G. Wu, W. Dai and K. Fan, *J. Catal*. 2007, **246**, 193.
27. H. Castricum, H. Bakker, B. van der Linden and E. K. Poels, *J. Phys. Chem. B*, 2001, **105**, 7928.
28. J. Rakoczy, J. Nizioł, K. Wieczorek-Ciurowa and P. Dulian, *React. Kinet., Mech. Catal*., 2013, **108**, 81.
29. (a) R. Zhang, A. Villanueva, H. Alamdari and S. Kaliaguine, *J. Catal*., 2006, **237**, 368; (b) R. Zhang, A. Villanueva, H. Alamdari and S. Kaliaguine, *Appl. Catal., B*, 2006, **64**, 220; (c) R. Zhang, A. Villanueva, H. Alamdari and S. Kaliaguine, *Appl. Catal., A*, 2006, **307**, 85; (d) R. Zhang, H. Alamdari and S. Kaliaguine, *Appl. Catal., A*, 2008, **340**, 140.
30. D. W. Kwon, K. H. Park and S. C. Hong, *Appl. Catal., A*, 2013, **451**, 227.
31. L. Ilieva, G. Pantaleo, I. Ivanov, R. Zanella, A. M. Venezia and D. Andreeva, *Int. J. Hydrogen Energy*, 2009, **34**, 6505.
32. L. Ilieva, G. Pantaleo, I. Ivanov, A. Maximova, R. Zanella, Z. Kaszkur, A. M. Venezia and D. Andreeva, *Catal. Today* 2010, **158**, 44.
33. D. Andreeva, I. Ivanov, L. Ilieva, J. Sobczak, G. Avdeev and K. Petrov, *Top. Catal*. 2007, **44**, 173.
34. D. Fino, N. Russo, G. Saracco and V. Specchia, *J. Catal*. 2006, **242**, 38.
35. (a) W. Tong, A. West, K. Cheung, K.-M. Yu and S. C. E. Tsang, *ACS Catal*. 2013, **3**, 1231; (b) N. Sun, X. Wen, F. Wang, W. Wei and Y. Sun, *Energy Environ. Sci*. 2010, **3**, 366.
36. S. S. Acharyya, S. Ghosh, R. Tiwari, B. Sarkar, R. K. Singha, C. Pendem, T. Sasaki and R. Bal, *Green Chem*. 2014, **16**, 2500.
37. (a) Y. Tanaka, T. Utaka, R. Kikuchi, T. Takeguchi, K. Sasaki and K. Eguchi, *J. Catal*. 2003, **215**, 271; (b) E. Manova, D. Paneva, B. Kunev, C. Estournès, E. Rivière, K. Tenchev, A. Léaustic and I. Mitov, *J. Alloys Comp*. 2009, **485**, 356.
38. E. Manova, T. Tsoncheva, D. Paneva, I. Mitov, K. Tenchev and L. Petrov, *Appl. Catal., A*, 2004, **277**, 119.
39. N. Velinov, K. Koleva, T. Tsoncheva, E. Manova, D. Paneva, K. Tenchev, B. Kunev and I. Mitov, *Catal. Commun*., 2013, **32**, 41.
40. J.C. Colmenares, R. Luque, *Chem. Soc. Rev.* 2014, **43**, 765.
41. P. Billik, G. Plesch, V. Brezova, L. Kuchta, M. Valko and M. Mazur, *J. Phys. Chem. Solids* 2007, **68**, 1112.
42. (a) S. Yin, H. Yamaki, M. Komatsu, Q. Zhang, J. Wang, Q. Tang, F. Saito and T. Sato, *J. Mater. Chem*. 2003, **13**, 2996; (b) S. Yin, H. Yamaki, Q. Zhang, M. Komatsu, J. Wang, Q. Tang, F. Saito and T. Sato, *Solid State Ionics* 2004, **172**, 205.
43. (a) S. F. Chen, L. Chen, S. Gao and G. Y. Cao, *Chem. Phys. Lett*. 2005, **413**, 404; (b) Y.-C. Tang, X.-H. Huang, H.-Q. Yu and L.-H. Tang, *Int. J. Photoenergy* 2012, 960726.
44. S. Yin, M. Komatsu, Q. Zhang, F. Saito and T. Sato, *J. Mater. Sci*. 2007, **42**, 2399.
45. S. Yin, H. Hasegawa, D. Maeda, M. Ishitsuka and T. Sato, *J. Photochem. Photobiol*. A 2004, **163**, 1.
46. Q. Zhang, J. Wang, S. Yin, T. Sato and F. Saito, *J. Am. Ceram. Soc*. 2004, **87**, 1161.
47. J. Wang, S. Yin, Q. Zhang, F. Saito and T. Sato, *J. Mater. Chem*. 2003, **13**, 2348.
48. A. Betke and G. Kickelbick, *New J. Chem*. 2014, **38**, 1264.
49. S. K. Pardeshi and A. B. Patil, *J. Mol. Catal. A: Chem*. 2009, **308**, 32.
50. M. Francavilla, A. Pineda, A.A. Romero, J.C. Colmenares, C. Vargas, M. Monteleone, R. Luque, *Green Chem*. 2014, **16**, 2876.
51. A. Diez-Pascual, C. Xu, R. Luque, *J. Mater. Chem. A* 2014, **2**, 3065.
52. A. Dodd, A. McKinley, M. Saunders and T. Tsuzuki, *Nanotechnology* 2006, **17**, 692.
53. X. L. Guo, H. Tabata and T. Kawai, *J. Cryst. Growth* 2002, **237**, 544.
54. K. Nakahara, H. Takasu, P. Fons, A. Yamada, K. Iwata, K. Matsubara, R. Hunger and S. Niki, *Appl. Phys. Lett*., 2001, **79**, 4139.
55. X. Wang, S. Yang, J. Wang, M. Li, X. Jiang, G. Du, X. Liu and R. P. H. Chang, *J. Cryst. Growth* 2001, **226**, 123.
56. J. Lu, Q. Zhang, J. Wang, F. Saito and M. Uchida, *Powder Technol*., 2006, **162**, 33.
57. N. Linares, E. Serrano, M. Rico, A.M.Balu, E. Losada, R. Luque, J.García-Martínez, *Chem. Commun*. 2011, **47**, 9024.
58. (a) A. Pineda, A. M. Balu, J. M. Campelo, A. A. Romero, D. Carmona, F. Balas, J. Santamaria and R. Luque, *ChemSusChem*, 2011, **4**, 1561; (b) A. Pineda, A. M. Balu, J. M. Campelo, R. Luque, A. A. Romero, J. C. Serrano-Ruiz, *Catal. Today*, 2012, **187**, 65; (c) R. Hosseinpour, A. Pineda, A. Garcia, A. A. Romero, R. Luque, *Catal. Commun*. 2014, **48**, 73.
59. (a) A. Toledano, L. Serrano, J. Labidi, A. M. Balu, A. Pineda and R. Luque, *ChemCatChem*, 2013, **5**, 977; (b) A. Toledano, L. Serrano, A. Pineda, A. M. Balu, R. Luque and J. Labidi, *ChemSusChem*, 2013, **6**, 529.
60. A. Toledano, L. Serrano, A. Pineda, A. A. Romero, R. Luque and J. Labidi, *Appl. Catal. B: Environ*., 2014, **145**, 43.
61. (a) M. Ojeda, A. M. Balu, V. Barron, A. Pineda, A. G. Coleto, A. A. Romero and R. Luque, *J. Mater. Chem. A*, 2014, **2**, 387; (b) M. Ojeda, A. Pineda, A. A. Romero, V. Barron, and R. Luque, *ChemSusChem*, 2014, **7**, 1876.
62. (a) A.-H. Lu, E. L. Salabas and F. Schuth, *Angew. Chem. Int. Ed*., 2007, **46**, 1222; (b) V. Polshettiwar and R. S. Varma, *Chem. Eur. J*., 2009, **15**, 1582; (c) V. Polshettiwar and R. S. Varma, *Green Chem*., 2010, **12**, 743; (d) S. Shylesh, V. Schunemann and W. R. Thiel, *Angew. Chem. Int. Ed*., 2010, **49**, 3428.
63. V. Polshettiwar and R. S. Varma, *Chem. Soc. Rev*., 2008, **37**, 1546.
64. A. Yepez, A. Pineda, A. Garcia, A. A. Romero and R. Luque, *Phys. Chem. Chem. Phys.*, 2013, **15**, 12165.
65. M. Chidambaram, A.T. Bell, *Green Chem*. 2010, **12**, 1253.
66. G. Majano, L. Borchardt, S. Mitchell, V. Valtchev and J. Perez-Ramirez, *Microporous Mesoporous Mater*., 2014, **194**, 106.
67. A. Grau, R. Campos, E. Serrano, M. Ojeda, A.A. Romero, J. Garcia-Martinez, R. Luque, *ChemCatChem* 2014, **6**, 3530.
68. J. Xie and S. Kaliaguine, *Appl. Catal., A*, 1997, **148**, 415.

69. N. G. Kostova, A. A. Spojakina, E. Dutkova and P. Balaz, *J. Phys. Chem. Solids* 2007, **68**, 1169.
70. (a) H. Xin, J. Zhao, S. Xu, J. Li, W. Zhang, X. Guo, E. J. M. Hensen, Q. Yang and C. Li, *J. Phys. Chem. C* 2010, **114**, 6553; (b) D.-Y. Ok, N. Jiang, E. A. Prasetyanto, H. Jin and S.-E. Park, *Microporous Mesoporous Mater*. 2011, **141**, 2; (c) X. Wang, G. Li, W. Wang, C. Jin and Y. Chen, *Microporous Mesoporous Mater*. 2011, **142**, 494; (d) Y. Qi, C. Ye, Z. Zhuang and F. Xin, *Microporous Mesoporous Mater*. 2011, **142**, 661.
71. (a) K. Yamamoto, S. E. B. Garcia and A. Muramatsu, *Microporous Mesoporous Mater*. 2007, **101**, 90; (b) S. Garcia, K. Yamamoto, F. Saito and A. Muramatsu, *J. Jpn. Pet. Inst*. 2007, **50**, 53.
72. T. Iwasaki, M. Isaka, H. Nakamura, M. Yasuda and S. Watano, *Microporous Mesoporous Mater*. 2012, **150**, 1.
73. (a) T. Cassagneau, J. H. Fendler, S. A. Jonhson and T. E. Mallouk, *Adv. Mater*. 2000, **12**, 1363; (b) J. Xu, Y. Hu, L. Song, Q. Wang, W. Fan and Z. Chen, *Carbon* 2002, **40**, 445.
74. Y. H. Chu, Z.-M. Wang, M. Yamagishi, H. Kanoh, T. Hirotsu and Y.-X. Zhang, *Langmuir* 2005, **21**, 2545.
75. S. Li, Y. Wang, C. Lai, J. Qiu, M. Ling, W. Martens, H. Zhao and S. Zhang, *J. Mater. Chem. A* 2014, **2**, 10211.
76. M. Balaz, P. Balaz, G. Tjuliev, A. Zubrik, M.J. Sayagues, A. Zorkovska, N. Kostova, J. Mater. Sci. 2013, 48, 2424.
77. T. Xing, J. Sunarso, W. Yang, Y. Yin, A. M. Glushenkov, L. H. Li, P. C. Howlett and Y. Chen, *Nanoscale* 2013, **5**, 7970.
78. H-C. Zhou, J.R. Long, O.M. Yaghi, *Chem. Rev*. 2012, **112**, 673 and references therein.
79. S. T. Meek, J. A. Greathouse , and M. D. Allendorf, *Adv. Mater*. 2011, **23**, 249.
80. (a) J. Y. Lee, O. K. Farha, J. Roberts, K. A. Scheidt, S. T. Nguyen and J. T. Hupp, *Chem. Soc. Rev*., 2009, **38**, 1450; (b) A. Corma, H. Carcia and F. X. Llabres i Xamena, *Chem. Rev*., 2010, **110**, 4606.
81. a) A. Dhakshinamoorthy, H. Garcia, *ChemSusChem* 2014, **7**, 2392-2410; b) A. Dhakshinamoorthy, A.M. Asiri, H. Garcia, *Chem. Commun.* 2014, **50**, 12800-12814; c) A. Dhakshinamoorthy, H. Garcia, *Chem. Soc. Rev.* 2014, **43**, 5750-5765; d) A. Dhakshinamoorthy, M. Opanasenko, J. Cejka, H. Garcia, *Adv. Synth. Catal.* 2013, **355**, 247-268; e) A. Dhakshinamoorthy, H. Garcia, *Chem. Soc. Rev***.** 2012, **41**, 5262-5284.
82. A. Pichon, A. Lazuen-Garay and S. L. James, *CrystEngComm.* 2006, **8**, 211.
83. A. Pichon and S. L. James, *CrystEngComm*. 2008, **10**, 1839.
84. (a) P. J. Beldon, L. Fabian, R. S. Stein, A. Thirumurugan, A. K. Cheetham, T. Friscic, *Angew. Chem. Int. Ed*. 2010, **49**, 9640; (b) T. Friscic, D. G. Reid, I. Halasz, R. S. Stein, R. E. Dinnebier, M. J. Duer, *Angew. Chem. Int. Ed*. 2010, **49**, 712.
85. W. Yuan, T. Friscic, D. Apperley, and S. L. James, *Angew. Chem. Int. Ed*. 2010, **49**, 3916.
86. B. P. Biswal, S. Chandra, S. Kandambeth, B. Lukose, T. Heine and R. Banerjee, *J. Am. Chem. Soc*., 2013, **135**, 5328.
87. R. Li, X. Ren, H. Ma, X. Feng, Z. Lin, X. Li, C. Hu and B. Wang, *J. Mater. Chem. A* 2014, **2**, 5724.
88. S. Tanaka, K. Kida, T. Nagaoka, T. Ota and Y. Miyake, *Chem. Commun*. 2013, **49**, 7884.
89. (a) T. Friscic, I. Halasz, P. J. Beldon, A. M. Belenguer, F. Adams, S. A. J. Kimber, V. Honkimaki and R. E. Dinnebier, *Nat. Chem*. 2013, **5**, 66; (b) I. Halasz, S. A. J. Kimber, P. J. Beldon, A. M. Belenguer, F. Adams, V. Honkimaki, R. C. Nightingale, R. E. Dinnebier and T. Friscic, *Nat. Protoc.* 2013, **8**, 1718; (c) I. Halasz, T. Friscic, S. A. J. Kimber, K. Uzarevic, A. Puskaric, C. Mottillo, P. Julien, V. Strukil, V. Honkimaki and R. E. Dinnebier, *Faraday Discuss*. DOI: 10.1039/c4fd00013g.
90. (a) D. Gracin, V. Strukil, T. Friscic, I. Halasz and K. Uzarevic, *Angew. Chem. Int. Ed*. 2014, **53**, 6193; (b) M. Juribasic, K. Uzarevic, D. Gracin and M. Curic, *Chem. Commun*. 2014, **50**, 10287.
91. a) J.M. Campelo, D. Luna, R. Luque, J.M. Marinas, A.A. Romero, *ChemSusChem* 2009, **2**, 18; b) R.J. White, R. Luque, V. Budarin, J.H. Clark, D.J. Macquarrie, *Chem. Soc. Rev*. 2009, **38**, 481.
92. (a) V. Sepelak, S. Begin-Colin, G. Le Caër, *Dalton Trans.* 2012, **41**, 11927; (b) V. Sepelak, M. Myndyk, R. Witte, J. Röder, D. Menzel, R.H. Schuster, H. Hahn, P. Heitjans, K.D. Becker, *Faraday Discuss.* 2014, **170**, 121; (c) K.L. Da Silva, D. Menzel, A. Feldhoff, K. Kübel, M. Bruns, A. Paesano Jr., A. Düvel, M. Wilkening, M. Ghafari, H. Hahn, F.J. Litterst, P. Heitjans, K.D. Becker, V. Sepelak, *J. Phys. Chem. C* 2011, **115**, 7209.